Composites Science and Technology 72 (2012) 774–787

Contents lists available at SciVerse ScienceDirect

Composites Science and Technology

journal homepage: www.elsevier.com/locate/compscitech

# Carbon nanotube-based polymer composites: A trade-off between manufacturing cost and mechanical performance

Ilias G. Tapeinos [a], Angelos Miaris [b], Peter Mitschang [b], Nikolaos D. Alexopoulos [a,*]

[a] Department of Financial Engineering, University of the Aegean, 41 Kountouriotou Str., 82100 Chios, Greece
[b] Institut für Verbundwerkstoffe GmbH, Verarb Fungstechnik, Erwin-Schroedinger, Strasse 58, 67663 Kaiserslautern, Germany

ARTICLE INFO

*Article history:*
Received 21 October 2011
Received in revised form 7 February 2012
Accepted 12 February 2012
Available online 20 February 2012

*Keywords:*
A. Carbon nanotubes
A. Glass fibres
B. Mechanical properties
D. Rheology
E. Resin Transfer Moulding (RTM)

ABSTRACT

A methodology was devised to evaluate the newly-developed carbon nanotube reinforced polymer composites by means of mechanical performance and manufacturing cost. Glass fibre reinforced-epoxy composite plates were produced having different parameters: (a) three manufacturing processes, (b) geometrical dimensions, (c) carbon nanotubes concentration in the epoxy resin and finally (d) modified resin infusion temperature. Tensile coupons were machined out of the manufactured plates and their quasi-static mechanical properties were evaluated. Three cost models were developed to assess plates and tensile coupons manufacturing cost for each different case. Optimal values were evaluated for major manufacturing parameters, driving force being the mechanical properties of interest (quality) as well as their low manufacturing cost. It is demonstrated that the added cost to manufacture such nano-reinforced composites is attributed to increase strength on the expense of ductility; the main benefit of the carbon nanotube-based polymer composites seems to be their ability to be monitored. Almost 20% added cost is paid to attain this new function of piezo-resistivity for the RTM process, while this amount further increases for the non-automated processes such as the Hand Lay-up.



## 1. Introduction

During the last decades, there is a strong demand increase for composite materials; in the aircraft industry critical parameters are their high specific strength and generally their advanced mechanical properties. Glass fibre reinforced polymers are widely used in aeronautics; however one of the key parameters to increase their share market is to increase/maintain manufacturing quality while decreasing their cost. In critical aeronautical applications, quality is expressed via the presence or absence of structural faults (e.g. lack of infusion, porosity, etc.) in the composites generated during the manufacturing process. These faults are closely linked with mechanical properties (quality) and degrade them significantly, e.g. ultimate tensile strength and elongation to fracture.

An essential drawback for the widespread use of GFRPs is their increased manufacturing cost; several models were developed to simulate the different manufacturing processes and calculate respective manufacturing cost. Aircraft manufacturers aim to design aircrafts with the lowest possible direct operating cost (DOC), which includes cost for depreciation, insurance, landing fees and fuel consumption [1]. A methodology for a combined cost/weight optimization of aircraft components, thereby inputting the weight penalty parameter which governs the balance between manufacturing cost and weight has been described explicitly in [2]. Balance of cost/weight ratio was also spotted in different case studies, e.g. stiffened composite panels, fuselage frames and wings, etc. [3–5]. Different design variables and methodologies were examined in order to minimize cost and weight. Investigations should not be focused on the 'pure' weight reduction, but rather on a combined minimization of manufacturing cost and structural weight [6]. Manson and Bernet indicated that developed cost estimation procedures and consolidation models can be applicable to a wide variety of composite manufacturing processes [7]. However, interaction between cost and consolidation models allows the determination of the necessary processing parameters to achieve the desired quality at a minimum manufacturing cost.

Optimization of composite manufacturing processes can occur with regard to the flow of process steps to manufacture integrated structures, e.g. for the case of an automotive floor pan [8]. The critical part of optimization is to carefully select the estimation variables, e.g. for the case of a composite waved beam using the autoclave cure [9]. Estimation of manufacturing costs of a simple component in a number of different composite materials and by following different manufacturing routes had been extensively analyzed in [10]. Park et al. calculated mould filling time using different injection gate locations in the case of Resin Transfer Mould-

* Corresponding author.
*E-mail address:* nalexop@aegean.gr (N.D. Alexopoulos).

0266-3538/$ - see front matter © 2012 Elsevier Ltd. All rights reserved.
doi:10.1016/j.compscitech.2012.02.004

**Nomenclature**

*Layup data*
$PAA$ ($m^2$) total part area
$WP$ (kg) weight of part
$NPL$ (/) number of plies
$WPL$ (kg) weight of each ply
$RWA$ (kg) weight of resin base case
$RWB$ (kg) weight of resin hardener case
$TRA$ (kg) total release agent per container
$CUI$ (–) CNTs unit of issue
$ARU_x$ ($m^2$) area of unit used

*Process data*
$RU_x$ (kg) resin used
$T$ (min) minutes per ($i$) procedure (labour or machine operation)
$t_{fill}$ (min) mould filling time for VARI and RTM
$t_{imp}$ (min) fibre impregnation time for Hand Lay-up
$n_A$ viscosity of resin base
$n_B$ viscosity of resin hardener
$n_{(A,B)}$ viscosity of mixture base and hardener
$CCON$ (wt.%) CNTs concentration
$F_{scrap}$ scrap allowance per i procedure
$CAP$ (kW) capacity installed at the equipment
$CF$ (/) fraction of the used electrical capacity to the installed capacity
$N_{pc}$ (/) number of pieces produced per year
$L_f$ (years) estimated life of equipment
$RA$ (kg) release agent used

*Materials cost data*
$C_r$ (cu) cost of the releasing agent
$PP$ (cu/unit) purchase price
$C_{fab}$ (cu) cost of the fabric
$C_{ind}$ (cu/kW h h) cost of industrial energy consumption per hour (kW h)
$C_{rfx}$ (cu) cost of release film
$C_{resa}$ (cu) cost of resin base
$C_{resb}$ (cu) cost of resin hardener
$C_{stx}$ (cu) cost per stage $x$
$C_{CNT}$ (cu) cost of CNT's unit of issue
$C_{TOTAL}$ (cu) total cost

*Labour cost data*
$LCD$ (cu/day) labour cost per day
$C_w$ (cu/h) cost of the specialized worker per hour (labour hourly rate)
$C_{wm}$ (cu/min) cost of the specialized worker per minute
$WHD$ (/) working hours per day

ing (RTM) method [11]. A correlation between mould filling time and manufacturing cost could be established and therefore manufacturing optimization can also be considered for this specific case. Processing parameters that minimized mould filling time for a given geometry of a structure were considered as optimal [12].

Use of carbon nanotubes (CNTs) in polymer composites has attracted great attention nowadays due to their excellent mechanical and electrical properties, e.g. [13,14]. Using resin reinforced with CNTs, a non-conductive GFRP composite can now become electrically conductive. Therefore, exploiting the methodology of Schulte and Baron [15] with the electrical resistance change of the electrically conductive CFRPs, GFRPs can now be monitored by measuring simultaneously surface electrical resistance change of a coupon during mechanical loading. Therefore, the addition of electrically conductive CNTs offers to non-conductive GFRP composites the potential for sensing capabilities through changes in electrical resistance on the onset of damage e.g. [16,17]. Multi-walled carbon nanotubes (MWCNTs) exhibit high potential for an electrical modification of polymers because of their balanced properties and good process ability in terms of easy dispersion [18]. MWCNTs had been used in polymer composites for sensing purposes and it was proved that also provided enhanced fracture properties e.g. [17–19].

Research on these newly-developed, multi-functional materials is mainly focused on the enhancement of their mechanical performance as well as measurements of electrical resistance change simultaneously recorded from stress/strain variances of the testing specimens, e.g. [13,20–22]. However, their fundamental rheological aspects, such as non-linear viscosity results in the continuous flows, have been scarcely reported, e.g. [23–26]. The critical parameters of rheological properties of the epoxy resin reinforced CNTs and their effects on processing and mechanical features of these composites have been scarcely studied in [27,28]. Nevertheless, a complete study on the global benefits of the addition of the CNTs in the composites by means of quality to cost ratio has not yet reported.

In the present work, an assessment of GFRPs reinforced with different percentages of CNTs in their epoxy matrix will be performed by means of mechanical and economical point of view. Different manufacturing processes of the new, innovative composites will be briefly described. Fully-parametric cost models for different processes and parameters of composite plates' manufacturing will be developed. Mechanical properties of the produced materials will be evaluated. Optimum manufacturing parameters will be post-identified, with regard to enhanced mechanical performance (quality) and low cost, produced through the most efficient manufacturing methods known so far.

## 2. Cost estimation background and methodology

Cost models will be developed to simulate manufacturing cost on GFRP composites, incorporating different parameters: (a) various manufacturing processes, (b) weight percentage of CNTs in epoxy resin, (c) resin infusion temperature and (d) plate's geometrical dimensions. For this cause, each manufacturing stage was divided in multiple sub-processes to better monitor them, while cost drivers were built up and associated with each sub-process. The cost drivers were related using Cost Estimation Relationships (CERs) in order to describe and relate effectively all activities throughout the GFRP manufacturing process.

Cost estimation approach in the present work will be based on the Activity Based Costing (ABC) method [29]; fundamental calculation flow diagram can be seen in Fig. 1. ABC methodology lies on the following steps:

(a) identification of activities or transactions that generate costs during product development (sub-processes and main processes),
(b) identification of cost drivers associated with each sub-process,
(c) assignment of costs to each sub-process via the creation of the Cost Estimation Relationships (CERs), and finally

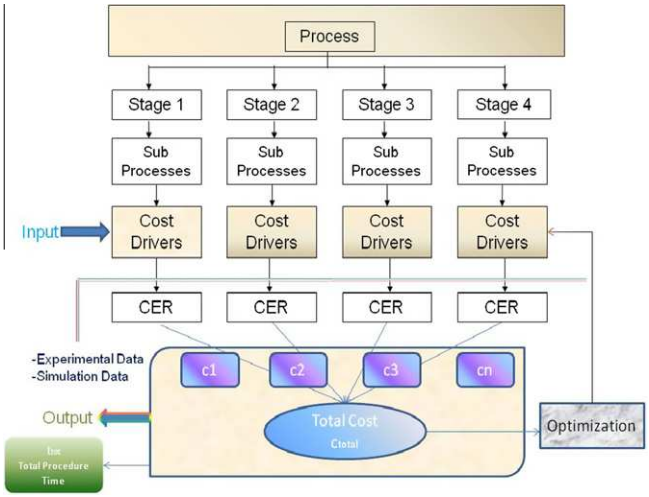


**Fig. 1.** Activity Based Costing (ABC) method loop.

(d) summation of the costs of sub-processes that occur to 'make' a product.

Methodology approach can be schematically seen in Fig. 2. Three different processes were cost-analyzed and composite plates were produced. A fast assessment via quality and cost showed the most efficient process under these fundamental criteria. Major manufacturing drivers were isolated to identify the individual optimal parameters for high quality and low cost of composites.

## 3. Composite manufacturing processes

GFRP plates were manufactured using three different methods; (a) Vacuum Assisted Resin Infusion, (b) Hand Lay-up and (c) Resin Transfer Moulding. All GFRP manufacturing processes will be shortly described and divided at stages to examine each process more effectively, thus enabling the identification of activities that generate costs at each process and calculate total manufacturing cost.

### 3.1. Vacuum Assisted Resin Infusion method

This section will describe all manufacturing steps of composites in Vacuum Assisted Resin Infusion (VARI) method. A timely arranged log, recording of all procedure steps is maintained, accompanied by cost and time estimates for materials used throughout, the process. The whole manufacturing process can be divided into four different sub-processes:

i. CNTs mixing stage,
ii. preparation and lay-up of the composite,
iii. main process resin infusion, and
iv. post processing – post curing.

Briefly, a short description of each different manufacturing stage will be given for the convenience of the reader.

#### 3.1.1. CNTs STAGE: preparation and mixing of CNTs

At this sub-process, different concentrations of CNTs per weight were added and dispersed in the epoxy resin. CNTs type was chosen to be multi-walled carbon nanotubes (MWCNTs) from Arkema, France-TNMH3, of diameter 10–20 nanometres (nm), while epoxy resin used was a typical aeronautical epoxy resin Araldite LY564/hardener Aradur 2954 supplied by Hunstman Advanced Materials, Bergkamen, Germany (ratio 100:35 parts by weight). Dispersion of MWCNTs in epoxy matrix had been performed via a Torus Mill™ dissolver (VMA, Getzmann GmbH), in the Advanced Composites Laboratory of Hellenic Aerospace Industry, Schimatari, Greece. Dispersion of CNTs in the epoxy resin was achieved via high shear forces of a high speed rotating disc to dissolve any formed agglomerates. More details regarding shear mixing, the effect of CNT concentration in agglomerate formation as well as in mechanical properties of nano-reinforced resin can be found in [22].

#### 3.1.2. STAGE 1: preparation

Layout of this stage can be seen in Fig. 3a. Plate manufacturing process is summarized as: ten (10) layers of fabric – type 1543 S2 style 6781 cross-woven fabric FIBERGLASS – oriented at 0/90° had been cut at the required square dimensions (e.g. 300 mm × 300 mm). The layers (area weight of fibres was

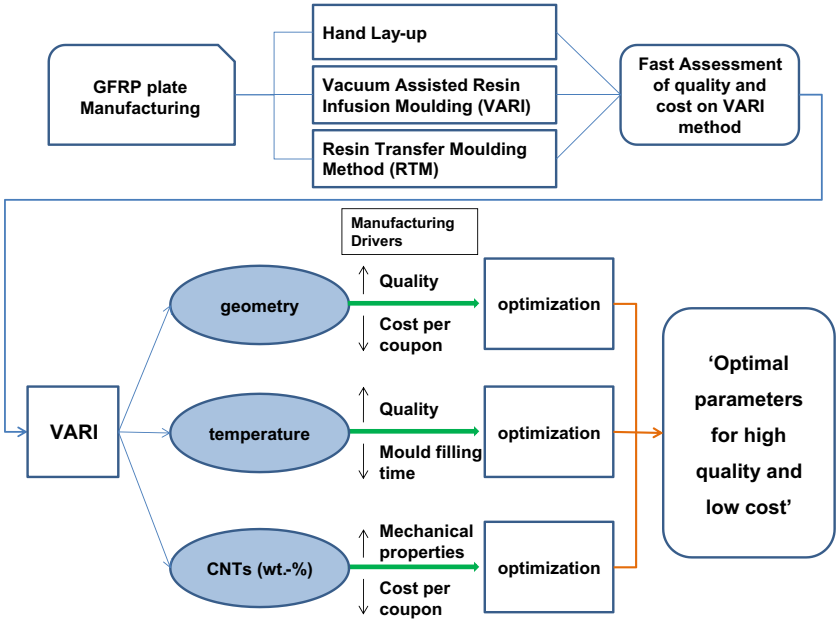


**Fig. 2.** Processing flow diagram of the proposed methodology for identification of optimum GFRP manufacturing parameters.

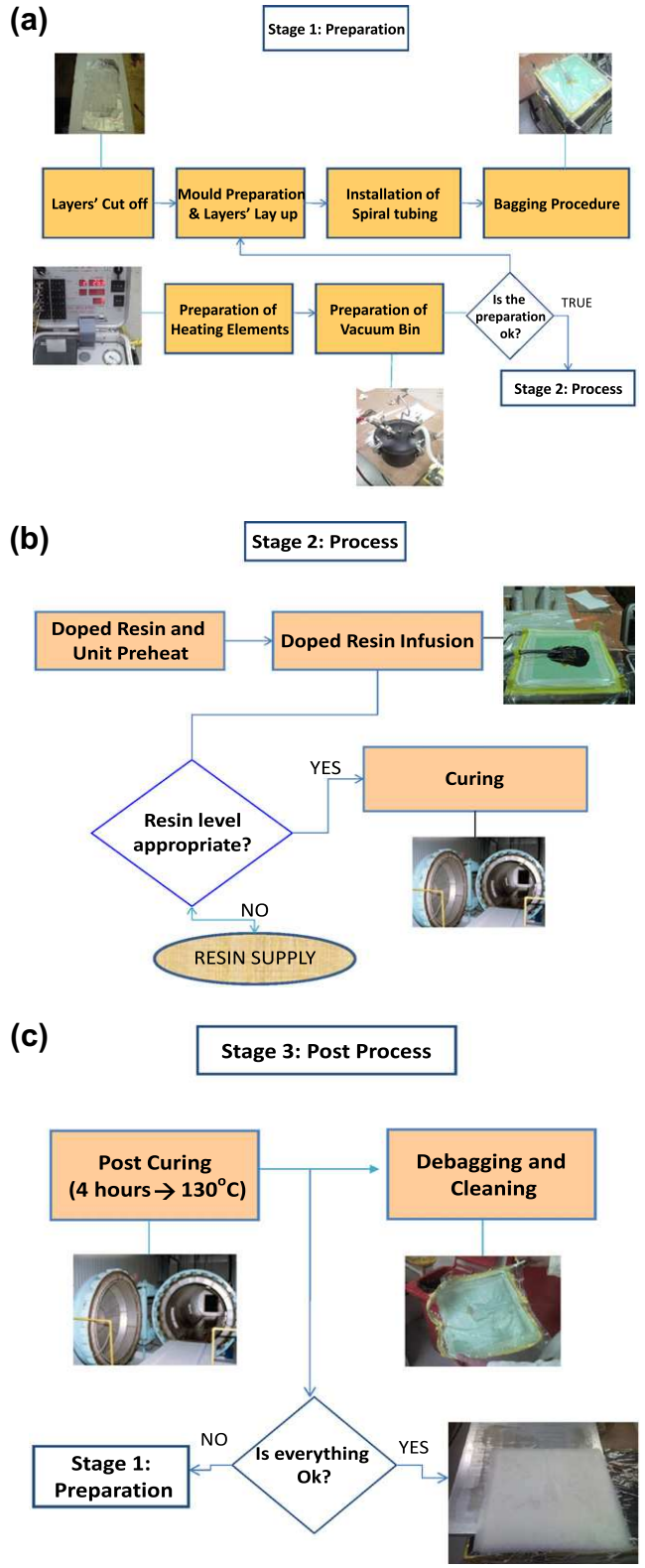


**Fig. 3.** Vacuum Assisted Resin Infusion (VARI) manufacturing process stages: (a) preparation, (b) main process and (c) post process stages loop.

0.298 kg/m$^2$) were set up with a parallel stacking sequence and placed inside the square mould. Vacuum bag moulding material had been used to eliminate entrapped air and excess resin. Appropriate bagging material was placed and vacuum conditions were applied and their sub-process finishes, just before the resin infusion.

*3.1.3. STAGE 2: main process*

This stage consists of the following sub-processes: resin preparation and mould preheat as well as resin injection at the unit followed by the curing procedure, Fig. 3b. Mould is preheated for half an hour at 50 °C by exploiting the appropriate heating monitoring system with thermocouples with the use of the ANITA GMI 9701 model, under vacuum. Resin manufacturer instructions were followed for the epoxy resin polymerization.

*3.1.4. STAGE 3: post process*

The analytical layout of this stage can be seen in Fig. 3c. It mainly consists of post curing of composite, as recommended by the resin manufacturer's data sheet. Debagging of the vacuum bagging material that was used on top of the mould takes place, as well as cleaning of the workbench.

*3.2. Hand Lay-up method*

This method consists of the use of an open mould and the resin is poured and brushed over and into the glass plies instead of being injected inside a closed mould. Entrapped air is removed manually with squeegees or rollers to complete the laminates structure. It is regarded as a quite simple – labour intensive method suited especially for large components. A significant aspect of Hand Lay-up is the absence of machines during fibre impregnation along with low cost tooling. The method was also divided into four stages: Stage 0 – CNTs mixing stage, Stage 1-Preparation, Stage 2-Process (manual resin application) and Stage 3-Post Process (post curing).

*3.3. Resin Transfer Moulding method*

Resin Transfer Moulding (RTM) is considered to be the most precise manufacturing process of composites but at the same time one of the most expensive due to machining cost of the metallic moulds and their high depreciation value. In addition, pre-processing time is higher when compared to the other processes due to mould preparation and pressure machine setup. The first step of this method is the CNTs mixing stage, which is a common step on all three manufacturing processes before the initiation of the preparation stage. As soon as CNTs mixing stage is over, the preparation of the closed mould begins. The second stage is regarded as the process of resin injection inside the closed mould from the source container through pressure application on the source container. At last, the third and final stage is the post curing of the unit, according to the resin manufacturer's data sheet.

## 4. Experimental procedure

GFRP plates were manufactured at the required square dimensions (e.g. plate edges: 300 mm, 400 mm, 500 mm, 600 mm, 800 mm and 1000 mm), either with neat epoxy resin or doped resin with CNTs at various concentrations (e.g. 0.5 wt.%, 0.75 wt.%, or 1.00 wt.%, etc.). Each plate consisted of 10 plies of cross woven fabric, oriented at 0/90°, while the area weight of fibres was 0.298 kg/m$^2$. Resin injection inside the mould was carried out for various temperatures (from 40 °C and up to 80 °C with a grid of 10 °C) in order to change its viscosity characteristics that have a strong effect on the mould filling time. A shear rheometer (rotational cylinder) in the Institut für Verbundwerkstoffe was used to measure resin solution viscosity in response to applied temperature. The resin solution was placed within the annulus of one cylinder inside another. One of the cylinders was rotated at a set speed, which

determines the shear rate inside the annulus. The value of shear rate applied was 1000 $s^{-1}$ which is in the range of testing for epoxy resins, e.g. [24,25]. The liquid tended to drag the other cylinder round, and the force it exerted on that cylinder was measured, which can be converted to a shear stress.

Cross section of tensile composite coupons had been cut in a rotary disc very carefully such as not to produce delamination and any other kind of damage to the specimen's surface for investigation. Leica light optical and JEOL scanning electron microscopes of Institut für Verbundwerkstoffe had been used to access and investigate the CNTs distribution through the composite specimen's thickness. Silver conductive paste was added at the cross section of coupons in order to enhance the analysis from the microscope.

Tensile specimens had been cut from plates according to the ASTM D3039 specification and edge-polished. The dimensions of the testing specimens were width × length = 25 mm × 250 mm. For the case of GFRP coupons with CNTs reinforcement in the resin, two (2) electrical cable connectors were also attached to the specimen surface. The cables were connected to an Agilent multimeter and the initial resistance of the reference test section was measured by means of two point measurements. A DC voltage of 10 V was applied to cables connected to the specimen surface; the current was measured and the resistance was calculated from these values. This configuration was established in order to seek the electrical response character, used for monitoring purposes. Testing of the 'hybrid' composites had been performed on the MTS 100 KN testing machine of Advanced Composites Laboratory of Hellenic Aerospace Industry. Axial monotonic tensile tests till fracture were conducted in the present work. A 50 mm extensometer was additionally attached to the opposite surface of the specimens; force, displacement, electrical resistance and strain from the extensometer measurements were recorded during the mechanical test and stored in to the P/C.

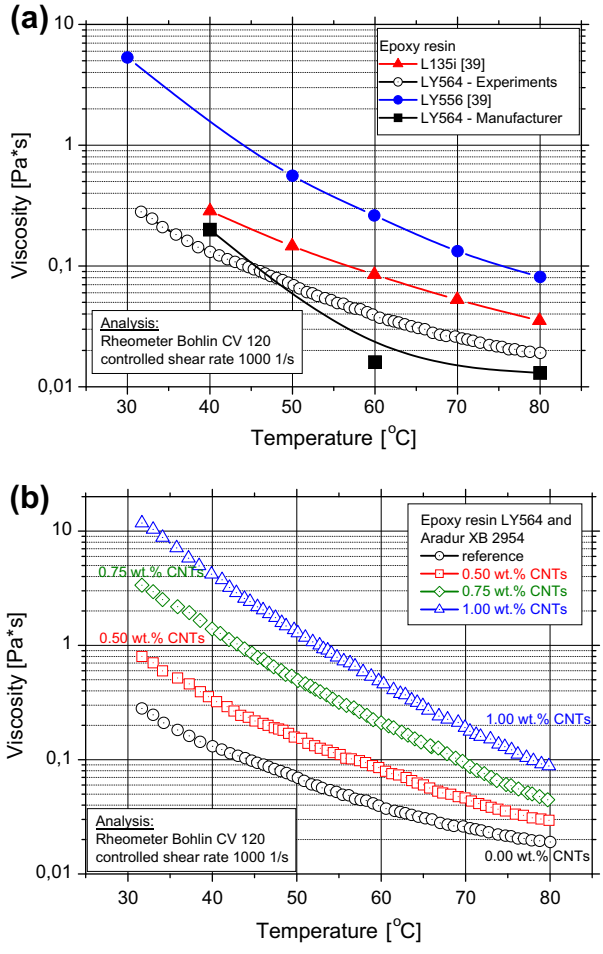


**Fig. 4.** (a) Exponential correlation of dynamic viscosity with temperature of epoxy resins and (b) effect of different wt.% CNTs addition on the viscosity of the epoxy resin LY564.

## 5. Experimental results

### 5.1. Viscosity tests

Fig. 4a shows the experimental results of the reference epoxy resin as a function of testing temperature. Resin flow is increasing with continuous increasing temperature up to 80 °C, which is the typical upper range shelf in order to be used for injection purposes in composites. Data of manufacturer were also added in the figure as well as other similar epoxy resins of the open literature. Acquired data was very convincing and all types of epoxy resins showed similar behaviour with the experiments.

The effect of CNTs addition in epoxy resin's LY564 viscosity can be seen in Fig. 4b. As expected, the CNTs addition at various concentrations increased the resin's viscosity. For example, the addition of 1.0 wt.% CNTs increased its viscosity by more than 100 times when compared to reference resin at 33 °C. As can be seen in Fig. 4b for the case of increasing testing temperature, the viscosity values of all four different materials is decreasing, thus the difference between reference and 1.0 wt.% CNTs resin being one order of magnitude at 80 °C. Of course, this will definitely affect the mould filling time, and this effect will be analyzed below.

### 5.2. Microscopical investigation

Microscopical evaluation results of specimens' cross section for a VARI manufactured 1.0 wt.% CNTs reinforced GFRP composite can be seen in Fig. 5. Fig. 5a illustrates a region where CNT agglomerates has occurred by the infiltration effect; in low magnification agglomerates are shown as white areas. Distribution of CNTs is not equally among the matrix; figure shows that CNTs tend to be located nearby reinforcing fibres, probably due to the filtration effect when trying to pass through fabrics during impregnation. Compared to lower CNT content composites it can be remarked that at higher CNT content, the CNTs are distributed less efficiently, thus probably affecting negatively the mechanical properties. Fig. 5b shows an area with efficient dispersion CNTs. Fig. 5c shows a higher magnification of areas of formed agglomerates and dispersed CNTs, while Fig. 5d shows how CNTs are not equally distributed and each individual CNT can be seen as a white spot. CNTs seem not to be distributed evenly at the matrix and this is one of the major concerns in the research community, e.g. [30,31].

### 5.3. Tensile tests

Tensile test results of the manufactured composites with different percentages of CNT doped resin can be seen in Fig. 6a. As expected, modulus of elasticity of nanocomposites was increased with increasing content of CNTs in the resin. Nevertheless, strain energy density – which represents the ability of the composite to absorb mechanical energy up to fracture point – is essentially decreased by almost 40% for the case of 1.0 wt.% doped resin composite. Tensile strength's increase $R_m$ is within the range of scatter of measured property; more details regarding tensile test and results can be found in [22]. What is more interesting is the addition of another function; the ability of the composite to be

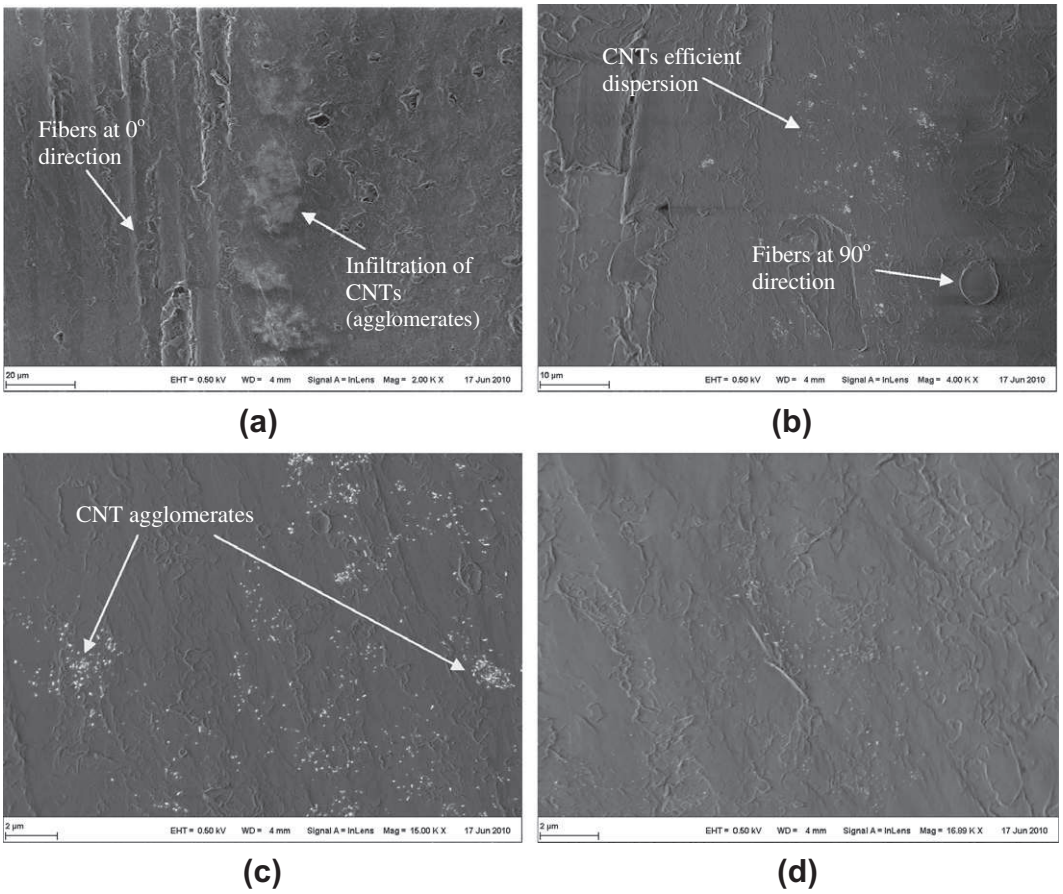


**Fig. 5.** SEM micrographs of produced CNT-based polymer composites specimens with 1.0 wt.% CNTs concentrations at different resolutions: (a) low resolution showing infiltration of CNT agglomerates, (b) area with more efficient CNT dispersion, (c) higher resolution of dispersed CNTs (each CNT can be seen as white dot) and (d) not equal distribution of CNTs in the resin matrix.

electrically monitored via its surface electrical resistance change. In Fig. 6b, one can notice both, the mechanical (in black) and electrical resistance (in blue) response of the composite for incremental loading – unloading tests of a 0.75 wt.% CNTs composite up to fracture. It can be seen that $\Delta R/R_0$ increases with increasing applied mechanical strain and decreases when unloading. In addition, it is quite clear that residual resistance occurs when unloading at higher strain levels, which is evidence of matrix cracking at the previous loading steps. Worth noting is that for the very low level of applied strain, no residual resistance occurs after unloading, thus at the very early stages ($\sim$50 MPa or 0.15% $\varepsilon$) no significant matrix damage occurred. More details regarding the piezo-resistivity effect can be found in [22] and in a forthcoming article of the authors.

A quality index that would reflect the materials ability for mechanical performance should address simultaneously for strength and ductility capabilities. Hence the effect of addition of CNTs should be counter measured, since an increase in one property is followed by a decrease in the other. Same effect was noticed on metallic materials, where application-specific quality indices were formed e.g. for cast aluminium alloys for aircraft applications [32], Transformation Induced Plasticity (TRIP) alloys [33] for automotive applications, as well as concrete reinforced bars for civil-engineering applications [34]. For the generation of such a quality index, a measure of strength was decided to be either modulus of elasticity $E$ or tensile strength $R_m$, while a measure of ductility was decided to be strain energy $W$ or elongation at fracture $A_m$. Both indices were calculated and similar results were obtained, as can be seen in Fig. 7. Quality by means of mechanical performance is decreasing with increasing CNT content; however this is an individual judgement that is almost counter-balanced by the new function gained by the new composites, to be monitored via electrical resistance change, which is explicitly analyzed in [14,19,22].

## 6. Cost estimation methodology of manufactured composites

Methodology and cost drivers are provided below to model each manufacturing process and set the pace of the techno-economical evaluation, while all equation elements units of measurement are defined at Nomenclature section. Each stage cost consists of material, labour and energy consumption costs as well as fixed depreciation charges of used fixed asset. Therefore each stage is analyzed into sub-processes to be monitored more efficiently, in order to obtain the total manufacturing cost of each different manufacturing process. Each manufacturing process involves CNT mixing, preparation, process and post-process stages, and most of the steps involved throughout each stage are common among the manufacturing processes. Therefore, current cost analysis is applied to all three manufacturing processes, with only a few cost drivers applied to a specific manufacturing process.

In order to calculate the labour cost, the basic assumptions followed were 7.5 working hours per day, 5 working days per week and that the employer's contribution on gross salary is 35%. Technician's cost per hour is labour cost per day (*LCD*), over working hours per day (*WHD*):

$$C_w = \frac{LCD}{WHD}. \quad (1)$$

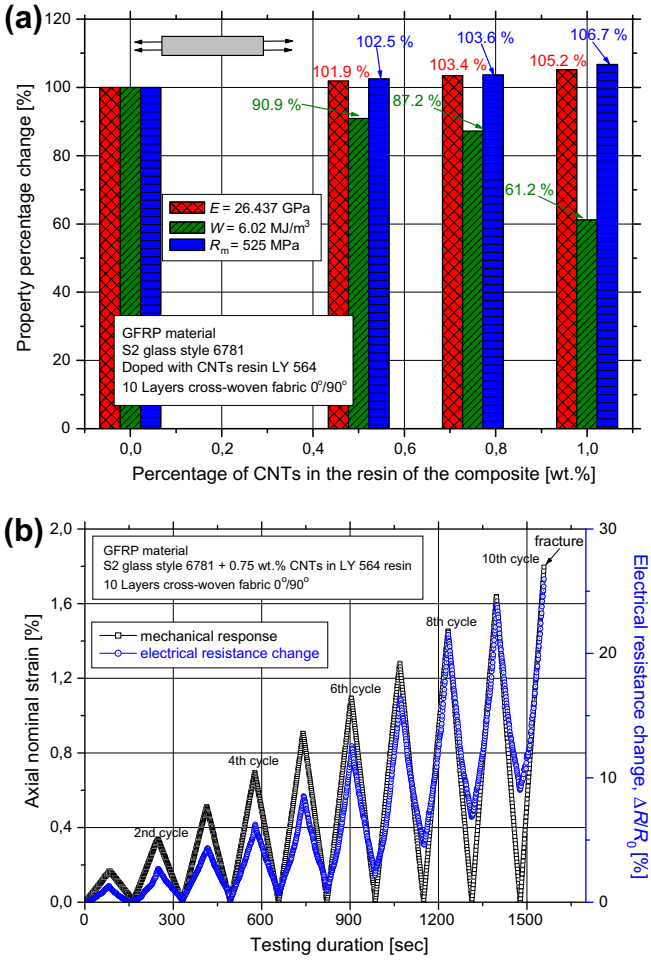


**Fig. 6.** (a) Percentage change of axial mechanical properties modulus of elasticity $E$, strain energy density $W$ and tensile strength $R_m$ due to the addition of CNTs in the resin matrix and (b) combined electrical and mechanical response of a 0.75 wt.% CNTs coupon (multi-functionality) to incremental loading – unloading tests.

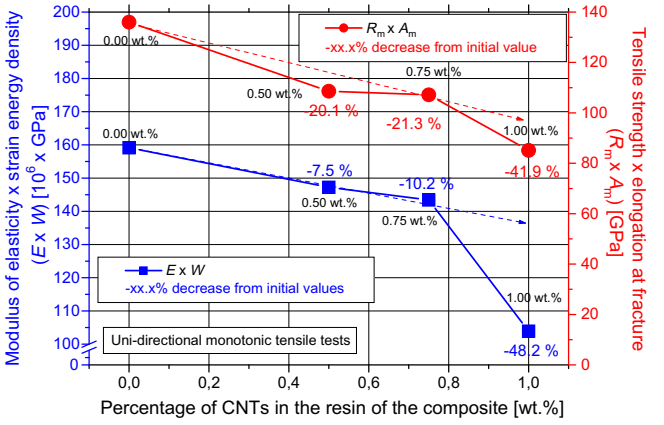


**Fig. 7.** Proposed quality indices by means of mechanical properties versus different CNTs percentage in the composite's matrix.

The technician's cost per minute is calculated as the quotient of Technician's cost per hour ($C_w$) over the number of minutes of an hour:

$$C_{wm} = \frac{C_w}{60}. \tag{2}$$

In the following, each stage will be presented separately and cost functions will be generated.

### 6.1. CNTs stage: CNTs preparation

Cost drivers were identified to assess total CNTs stage cost, namely on material cost $C_a$ and labour cost $C_b$. The following cost drivers of this section were applied to all manufacturing processes. Material cost of the CNTs dispersion stage is:

$$C_a = \frac{CCON \cdot (RUA + RUB) \cdot C_{CNT}}{CUI} + F_{scrap}, \tag{3}$$

where $CCON$ is CNTs concentration percentage, $RUA$ and $RUB$ define resin base and hardener weight accordingly, $C_{CNT}$ is the cost of CNTs case, $CUI$ is the CNTs number of units of issue and $F_{scrap}$ is the cost of material scrap. Material cost of resin base and hardener is allocated in the following stage 2. The labour cost of the CNTs dispersion stage is:

$$C_b = C_{wm} \cdot T(b), \tag{4}$$

where $C_{wm}$ is the labour cost per minute as calculated above and $T(b)$ is the total CNTs dispersion stage time. Energy consumption cost $C_c$ of the fixed asset used at this stage can be calculated as the product of:

$$C_c = CAP \cdot CF \cdot C_{ind} \cdot \frac{T(c)}{60}, \tag{5}$$

where $CAP$ is the installed capacity at the machine used at this step (in kW), $CF$ is the capacity range percentage of the machine, $T(c)$ is the total procedure machine minutes and $C_{ind}$ is the energy consumption cost per hour (in €). The fixed depreciation charge of the used fixed asset used throughout this stage is:

$$C_d = \frac{PP}{L_f \cdot N_{pc}}, \tag{6}$$

where $PP$ is the purchase price of the machine used at this step, $L_f$ is the number of years of estimated life of the machine used at this step and $N_{pc}$ describes the number of GFRP plates produced per year. Hence, total cost of CNTs stage is provided below as the sum of all the previous costs:

$$C_{CNT} = C_a + C_b + C_c + C_d. \tag{7}$$

### 6.2. STAGE 1: preparation

The first Stage is divided into various sub-processes. Each sub-process cost may consist of other costs, e.g. material, labour, energy and fixed depreciation charge.

#### 6.2.1. Layers' cut off

This sub-process consists of the cost of the material as well as labour cost of a Technician to cut the fabrics into the required dimensions. This is a common step among all three manufacturing processes and therefore the cost driver below was applied to them. Cost is calculated based on the formula:

$$\begin{aligned} C_1 &= C_{1mat} + C_{1labour} \\ &= \left(\frac{WPL \cdot NPL \cdot C_{fab}}{WP} + F_{scrap}\right) + C_{wm} \cdot T(1), \end{aligned} \tag{8}$$

where $T(1)$ is the time needed for the layers cut-off, $WPL$ is the single ply weight, $NPL$ is the number of plies used, $C_{fab}$ is the fabric roll total cost and $WP$ is the fabric roll total weight.

#### 6.2.2. Mould preparation and lay-up

The following cost driver was applied to all GFRP manufacturing processes because it consists of the activities to lay-up the fabrics

into the mould and to generally prepare it before the main process. Total cost of the mould preparation consists of:

$$C_2 = C_{2\text{mat}} + C_{2\text{labour}} = \left(\frac{RA \cdot C_r}{TRA} + F_{\text{scrap}}\right) + C_{\text{wm}} \cdot T(2), \quad (9)$$

where $T(2)$ is the time needed for the mould preparation and lay-up, $RA$ is the release agent used, $C_r$ is the cost of release agent and $TRA$ is the total weight of the release agent inside the case.

*6.2.3. Bagging procedure*

The cost drivers in this section were applied to VARI method only, mainly due to the fact that it consists of effort to bag the mould before resin infusion. Cut-off sub-process materials cost $C_3$ for bagging material is calculated as follows:

$$C_3 = C_{3\text{mat}} + C_{3\text{labour}} = \left(\frac{ARU_x \cdot C_{\text{rfx}}}{PAA} + F_{\text{scrap}}\right) + C_{\text{wm}} \cdot T(3), \quad (10)$$

where $T(3)$ is the time needed for bagging procedure, $ARU_x$ is the bagging film used, $C_{\text{rfx}}$ is the cost of bagging film and $PAA$ is the total part area. Therefore, total cost of Stage 1 for VARI method can be calculated as:

$$C_{\text{st1}} = C_1 + C_2 + C_3. \quad (11)$$

On the other hand, total cost of Stage 1 for Hand Lay-up and RTM can be calculated as:

$$C'_{\text{st1}} = C_1 + C_2 \quad (12)$$

*6.3. STAGE 2: process*

This stage consists of the cost of raw materials (resin and hardener) as well as preparation cost for processing. The following cost driver was applied to all manufacturing processes. Finally, curing costs are also included in this stage. Briefly, resin procedure cost $C_4$ is calculated as:

$$C_4 = (C_{\text{mat}} + C_{\text{labour}}) = \left[\left(\frac{RUA \cdot C_{\text{resa}}}{RWA} + \frac{RUB \cdot C_{\text{resb}}}{RWB}\right) + F_{\text{scrap}}\right] + C_{\text{wm}} \cdot T(4), \quad (13)$$

where $T(4)$ is the time needed for mixing of resin base and hardener, $RWA$ and $RWB$ are the resin base and resin hardener weight accordingly and $C_{\text{resa}}$ and $C_{\text{resb}}$ are the costs of the resin base and resin hardener, accordingly.

Energy consumption cost $C_c$ in this stage is calculated based on the installed capacity of the process depending on the $i$th procedure by exploiting Eq. (5) as well as the equipment depreciation charge per plate $C_d$ of the used fixed asset by exploiting Eq. (6). Below Eq. (14) can be applied to VARI and RTM methods only, since in Hand Lay-up no use of machinery is involved throughout the fibre impregnation and therefore only the labour cost was taken into account. Hence, resin injection cost $C_5$ for VARI and RTM depends on the mould filling time ($t_{\text{fill}}$) that will be defined and calculated below:

$$C_5 = t_{\text{fill.}} \cdot C_{\text{wm}} + CAP \cdot CF \cdot C_{\text{ind}} \cdot t_{\text{fill}} + C_d, \quad (14)$$

where $t_{\text{fill}}$ is the mould filling time and is being used instead of the symbol $T(5)$, while $C_d$ is the fixed depreciation charge of the used fixed asset used throughout RTM or VARI manufacturing processes. For the case of Hand Lay-up method, the cost driver would be:

$$C'_5 = t_{\text{imp}} \cdot C_{\text{wm}}, \quad (15)$$

where $t_{\text{imp}}$ is the fibre impregnation time for the Hand Lay-up method and is being used instead of the symbol $T(5)$. Curing process cost $C_6$ is a result of the energy consumption and fixed depreciation charge of the furnace used for the curing without any labour presence:

$$C_6 = CAP \cdot CF \cdot C_{\text{ind}} \cdot \frac{T(6)}{60} + C_d, \quad (16)$$

where $T(6)$ is the total time needed for the curing Stage 2 and $C_d$ is the fixed depreciation charge of the used fixed asset used for the curing process. The cost driver -given above- was applied to all three manufacturing processes. Total cost is calculated as the sum of the resin procedure cost, the resin injection cost and the curing cost. In specific, total cost for VARI and RTM processes would be:

$$C_{\text{st2}} = C_4 + C_5 + C_6, \quad (17)$$

while for the stage 2 of the Hand Lay-up method would be:

$$C'_{\text{st2}} = C_4 + C'_5 + C_6. \quad (18)$$

*6.4. STAGE 3: post process*

Cost driver $C_{\text{st3}}$ for the post curing step used at this step was based on Eq. (16) and was applied to all three manufacturing processes. The post processing step involves post curing of composite, as recommended by the resin manufacturer's data sheet, de-installation of all machinery used throughout the manufacturing process as well as cleaning of the workbench. This cost driver finally consists of:

$$C_{\text{st3}} = CAP \cdot CF \cdot C_{\text{ind}} \cdot \frac{T(7)}{60} + C_d, \quad (19)$$

where $T(7)$ is the total time needed for the post curing Stage 3 and $C_d$ is the fixed depreciation charge of the used fixed asset used for the post-curing process.

*6.5. Total cost*

Total cost of plate manufacturing for Hand Lay-up manufacturing process is the summation of costs from all employed sub-process stages:

$$C^1_{\text{TOTAL}} = C_{\text{CNT}} + C'_{\text{st1}} + C'_{\text{st2}} + C_{\text{st3}}, \quad (20)$$

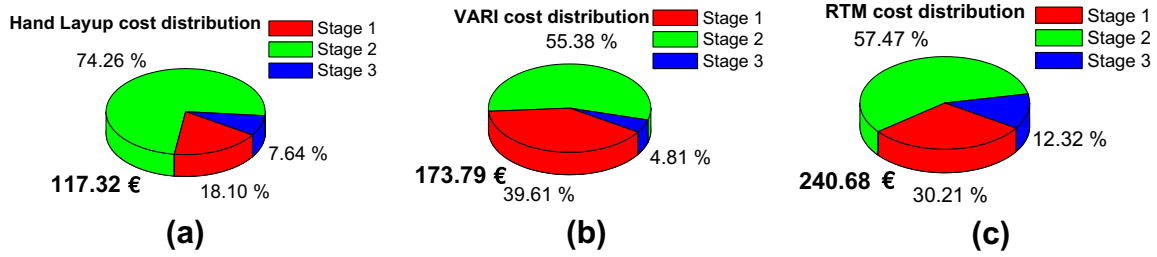


**Fig. 8.** Total cost and its distribution for (a) Hand Lay-up, (b) VARI and (c) RTM process for manufacturing of a reference 300 mm × 300 mm GFRP plate.

Furthermore, total cost of GFRP plate manufacturing for VARI method is:

$$C^2_{TOTAL} = C_{CNT} + C_{st1} + C_{st2} + C_{st3}, \quad (21)$$

Finally, total cost of GFRP plate using the RTM process is:

$$C^3_{TOTAL} = C_{CNT} + C'_{st1} + C_{st2} + C_{st3}. \quad (22)$$

## 7. Cost analysis

In this section, cost calculations have been performed for several different manufacturing cases and the calculation results will be shortly presented and analyzed.

### 7.1. Different manufacturing processes

Cost estimates were used to calculate and compare the cost behaviour of manufactured 'reference' (without any CNT addition) GFRP plates with three different manufacturing processes. Fig. 8 shows the cost distribution of all processes for manufacturing of a 300 mm × 300 mm GFRP plate using the neat epoxy resin. It can be shown that the least expensive GFRP manufacturing process is the Hand Lay-up method, mainly due to the absence of machinery or closed mould required for fibre impregnation with resin. Resin is applied manually by the technicians, which generates high labour costs. On the other hand, RTM is the most expensive but precise at the same process time, while VARI is the second least expensive process.

To this end, one has to notice that in high-mass production conditions, RTM is considered worldwide the most cost-efficient manufacturing method, mainly due to significant cut-down on

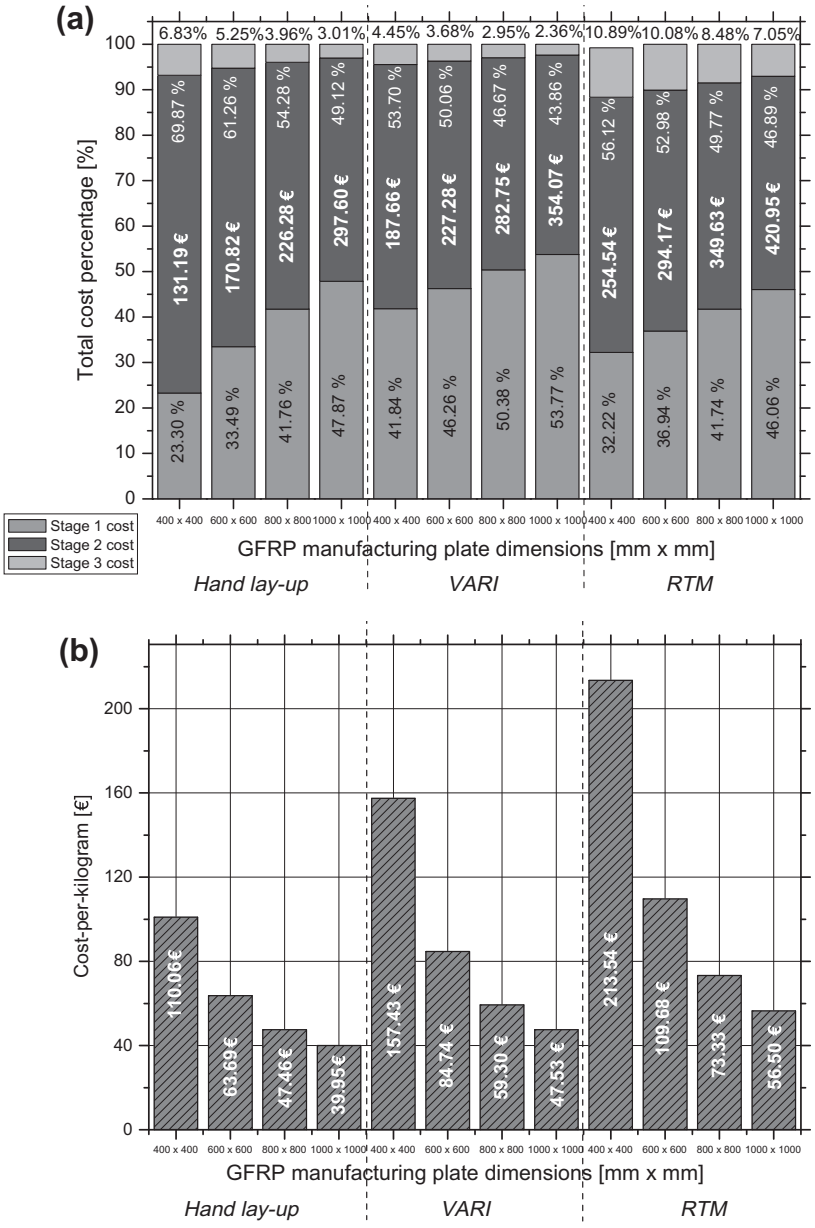


**Fig. 9.** (a) Cost distribution analysis for different manufacturing processes as well as geometrical dimensions and (b) cost per-kilogram analysis for different manufacturing processes as well as geometrical dimensions.

mould seal time and mould filling time [35]. Nevertheless, the results of the present work were the outcome of manufacturing GFRP plates under strict Laboratory conditions, and therefore Hand Lay-up and VARI methods are considered to require less time for machine setup for the manufacturing of a single GFRP plate. Perhaps this different ranking in terms of cost of the investigated manufacturing methods is due to the fact that the simulation was held for a continuous composites production and by exploiting available Laboratory infrastructure and not real, Industrial environment.

### 7.2. Different geometrical dimensions

Manufacturing cost is also a function of the composite structures' geometrical dimensions. Cost drivers revealed that the larger the plate dimensions, the lower the manufacturing cost per area, e.g. for the standard area of the tensile coupon. This is a result of the decreasing ratio between the fixed coupon size and the increasing GFRP surfaces. However, this might be the guide to misleading conclusions; at high manufactured GFRP dimensions, the allocation and adoption of the total cost at each coupon would be more efficient. Fig. 9a illustrates that as GFRP plate area grows, total manufacturing cost of each manufacturing process is increasing to a large extent. On the other hand, since a larger plate needs to be cut and placed inside the mould, preparation stage (stage 1) takes up a bigger share of the total cost for each of the three manufacturing processes, while process stage (stage 2) and post process (stage 3) costs are decreasing. Fig. 9b illustrates a comparison of Hand Lay-up, VARI and RTM on the basis of cost-per-kilogram of GFRP plates of various geometrical dimensions. It can be seen that as GFRP plate area grows, cost-per- kilogram of each manufacturing process is decreasing to a large extent, which can be accounted as a measure of the cost tendency when potentially manufacturing significantly larger GFRP plates. This enhances the argument of Fig. 8 that the least expensive GFRP manufacturing process is the Hand Lay-up method, VARI is the second least expensive process while RTM is the most expensive one and it denotes that the optimal geometrical dimension would be achieved in large GFRP plates.

### 7.3. Resin injection temperature and mould filling time

Stage 2 results (main process) showed that an essential parameter governing manufacturing cost is the mould filling time. It is well-known that mould filling time $t_{fill}$ is directly influenced by resin viscosity; viscosity of the resin mixture varies with injection temperature and CNTs concentration values and thus strongly influences mould filling time. Since the injected resin's viscosity is increasing, its diffusion rate inside mould is decreasing and thus mould filling time increases. A theoretical calculation of $t_{fill}$ will be attempted based on given geometrical dimensions and experimental viscosity values.

To this end, firstly the reinforcement's permeability tensors will have to be calculated; permeability is a property of the glass fabric and has a fixed value. Axial permeability $S_x$, through thickness permeability $S_z$ and transverse permeability $S_\psi$ of the woven fabric used can be expressed by employing the Kozeny-Carman equation [12]:

$$S_i = \frac{r_f^2 \cdot (1 - V_f)^3}{4 \cdot S_i \cdot V_f}, \quad \text{where } i = x, \psi, z. \tag{23}$$

In the above equation, $S_i$ is the permeability in each direction (in square meters), $r_f$ is the fibre radius (in meters), $V_f$ is the fibre volume fraction (in%) and $s_i$ is the Kozeny constant, which is direction dependant and can be calculated as:

$$(S_i)_{0/\theta} = (S_i)_{uni} \cdot \cos^2\theta + (S_i)_{0/90} + \cdot \sin^2\theta, \quad i = x, \tag{24}$$

$$(S_i)_{0/\theta} = (S_i)_{uni} \cdot \sin^2\theta + (S_i)_{0/90} + \cdot \cos^2\theta, \quad i = \psi, z. \tag{25}$$

In the above equation, $(s_i)_{uni}$ and $(s_i)_{0/90}$ are the Kozeny constants for flow transverse to the unidirectional fibre perform and for in-plane flow of a cross-woven (0/90°) structure, respectively. The constants take the theoretical values of $(s_x)_{0/\theta} = (s_x)_{uni} = 0.68$ and $(s_z)_{0/\theta} = (s_z)_{uni} = 11.0$ for cross woven fibre reinforcements (0/90°) [12]. However, $(s_\psi)_{0/90}$ takes the same value as $(s_x)_{0/90}$, while $(s_\psi)_{uni}$ is equal to $(s_z)_{uni}$ since the aligned fibre system is isotropic in the $\psi$–$z$ plane. Therefore, according to the literature [12] $(s_y)_{uni}$ and $(s_\psi)_{0/90}$ take the approximate values of 11.0 and 2.70, respectively.

In order to define the permeability sensors of the anisotropic preform, first the model of permeability of the isotropic needs to be calculated; square root of the multiplication of the two sensors $S_x$ and $S_\psi$ can be used [11]:

$$k_{iso} = \sqrt{S_x \cdot S_\psi}. \tag{26}$$

Application to symmetrical plates requires that the principal coordinate system will be transformed into a global-real coordinate system. The flow front is circular on an isotropic perform ($x$ and $\psi$ dimensions are the same), while an elliptical flow front was observed in the anisotropic preform and thus one of the $x$ or $\psi$ dimensions is larger than the other. The new coordinate system with $X$ and $\Psi$ being the new real elliptical dimensions (in m) consists of:

$$X = x \cdot \sqrt{\frac{k_{iso}}{S_x}} \quad \text{and} \quad \Psi = \psi \cdot \sqrt{\frac{k_{iso}}{S_\psi}}, \tag{27}$$

It is well-known that viscosity $\eta$(T) of a liquid varies (in Pa s) with temperature in a nonlinear manner, mainly exponential as can be seen in Fig. 4b; it can be calculated by employing an Arrhenius-type equation [36]:

$$\eta(T) = \eta_o \cdot \exp\left(\frac{Q(T)}{k_B \cdot T}\right), \tag{28}$$

where $\eta_o$ is a fixed viscosity value (in Pa s), $Q$(T) is the activation energy of the system as a function of temperature (in kJ/mol), $k_B$ is the molar gas constant (in $(m^2\ kg)/(K\ mol\ s^2)$) and $T$ is the resin injection temperature (in K). Taking the logarithm of Eq. (27), a linear regression can be used to calculate $\eta_o$ and $Q$(T) using the dynamic and isothermal experimental data concerning different viscosity values at different temperatures and before the gel point [37].

Calculation of mould filling time necessitates the pre-calculation of a certain fixed value $M$ that according to [11] consists of shear viscosity, fibre volume fraction and resin injection pressure as:

$$M = \frac{\eta(T) \cdot (1 - V_f) \cdot R_o^2}{4 \cdot k_{iso} \cdot p_o}, \tag{29}$$

where $p_o$ is the injection pressure (in bar) and $R_o$ is the radius of the inlet port. Mould filling time $t_{fill}$ for the radial flow of an anisotropic preform (in min) can be calculated by employing the formula proposed by Boccard et al. [38], as:

$$t_{fill} = M \cdot \left(\frac{r_{max}}{R_o}\right)^2 \cdot \left[2 \cdot \ln\left(\frac{r_{max}}{R_o}\right) + \left(\frac{R_o}{r_{max}}\right) - 1\right], \tag{30}$$

where $r_{max}$ is the maximum distance of the mould from the inlet port (in m).

Fig. 10a presents the mould filling time calculations for different GFRP plate sizes and resin infusion temperature using the VARI method. It is shown that at low resin injection temperature the mould filling time increases significantly. In addition, it is well-known that high resin injection temperature leads to resin gelation point that enhances resin shrinkage and generation of internal stress within the part. For this cause, 80 °C was assumed to be the upper shelf for injection temperature. Fig. 10b shows calculation results of mould filling time for various CNTs content (0.00, 0.50, 0.75 and 1.0 wt.%) and for infusion temperature values of 40, 50 and 60 °C. Increasing the CNT content leads to an increase in resin viscosity that according to [39] leads to a higher energetic efficiency of the dispersion process; however this has a negative effect on the mould filling time.

Fig. 11a shows the correlation among coupon costs for the various GFRP plate dimensions against varying resin injection temperatures. Coupons originated from GFRP plates with larger plate dimensions present lower cost when manufactured with higher resin injection temperature. However, the option of manufactured 1000 mm × 1000 mm GFRP plate is considered by the authors as non-valid, as it is difficult to maintain high quality (absence of structural faults) all over the plate and especially at locations near plate edges and the infusion gate (for the case of a single gate located at the centre of a square plate). In addition, infusion temperature of 80 °C was also rejected since a possible malfunction or over-shooting, injection temperature will cross

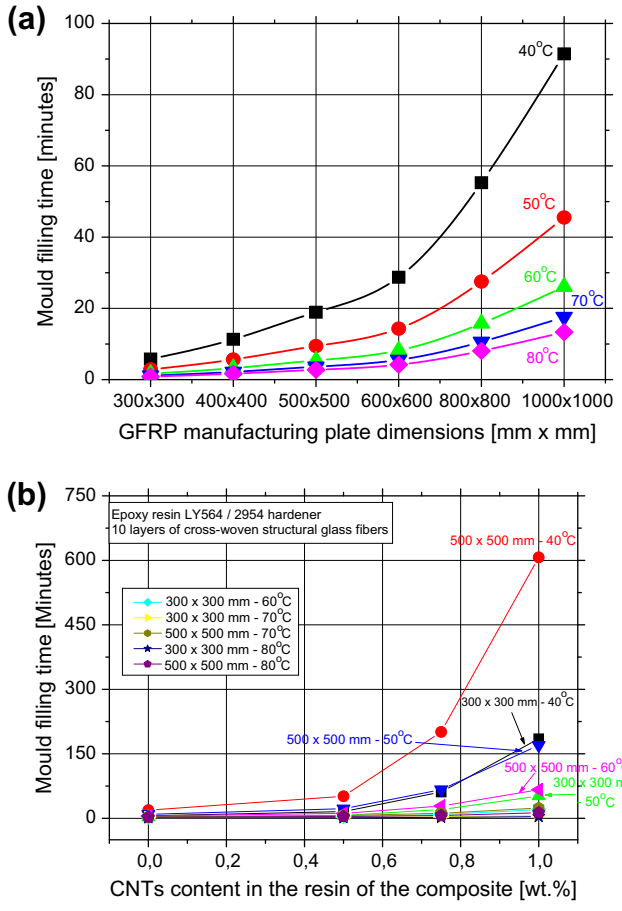


**Fig. 10.** (a) Mould filling time for different GFRP plate sizes using VARI method and (b) mould filling time for 300 mm × 300 mm and 500 mm × 500 mm GFRP plates and for various temperature values.

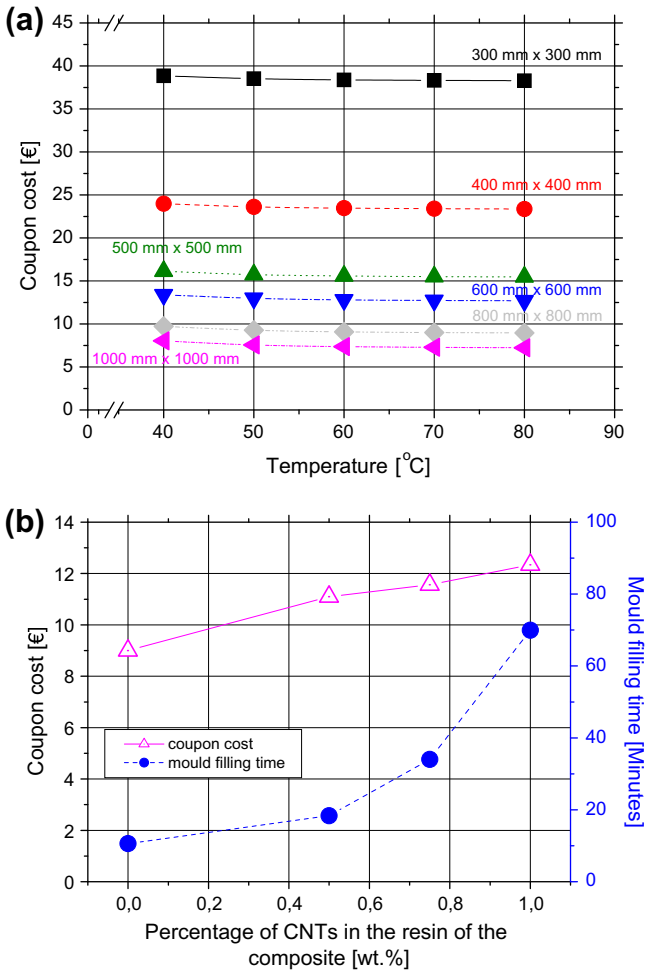


**Fig. 11.** (a) Correlation of the coupon cost to the resin injection temperature and (b) mould filling time and percentage of CNTs in the resin of the composite with 800 mm × 800 mm plate dimensions and with 70 °C as resin injection temperature.

the gelation point threshold that will quite degrade composite manufacturing quality. Therefore, the combination of resin injection temperature (70 °C) that minimizes mould filling time and does not lead to resin gelation and larger possible GFRP plate (800 mm × 800 mm) is considered to be the most promising for the specific case. Standard tensile coupon cost and mould filling time for the latter configuration can be seen in Fig. 11b. Although mould filling time and coupon cost show an increasing trend, their values remain significantly lower when compared to corresponding values at different GFRP plate areas and resin injection temperatures.

### 7.4. Addition of CNTs

CNTs addition altered resin viscosity properties; it was shown that with increasing CNTs content, resin flows more difficult for the same temperature, Fig. 4b. Fig. 12a shows cost calculation results for different manufacturing processes and CNTs content for the case of the most promising case of 800 mm × 800 mm plate at 70 °C resin infusion temperature. Addition of 0.50 wt.% CNTs results in a rapid increase of manufacturing cost as a result of additional material, labour, energy consumption and depreciation charge of the fixed assets used throughout the CNT and resin dissolving process. This was calculated to be approximate more than 20% of the total plate manufacturing cost. At higher CNT concentrations, manufacturing cost increases at a steady rate due to the fact

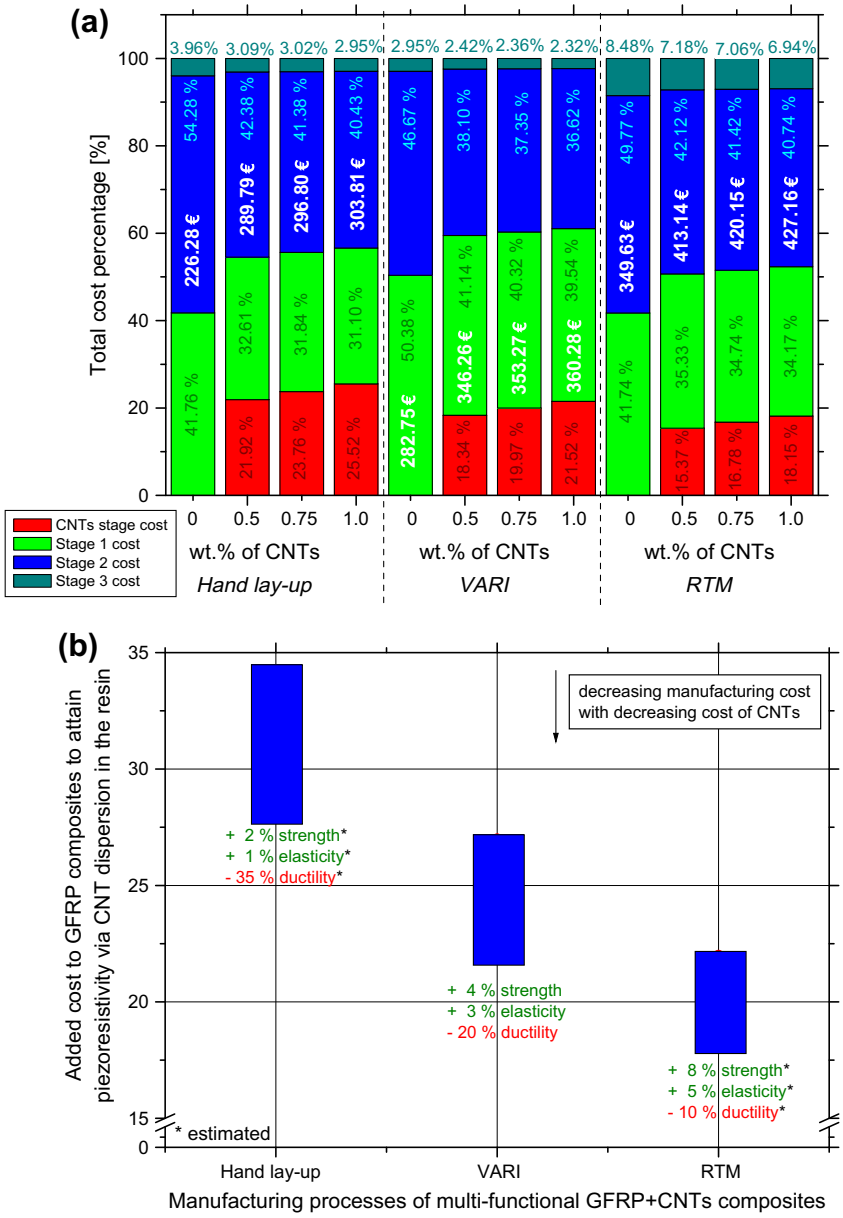


**Fig. 12.** (a) Cost distribution for all processes for the manufacturing of a GFRP plate with various CNTs concentrations with dimensions of 800 mm × 800 mm with 70 °C as resin injection temperature and (b) added percentage cost to attain piezoresistivity via the addition of CNTs in epoxy resin of GFRP.

that the only changing parameter is the material cost. Besides Hand Lay-up method, this was also the case for the VARI method; percentage of approximate 15% is noticed for this stage for the RTM due to its high manufacturing costs.

### 7.5. Cost to attain piezo-resistivity

There is a widespread belief in the academic community that the addition of CNTs deteriorates the mechanical performance (except of strength and fracture toughness) and adds manufacturing cost. To the authors' opinion, this can be counter-balanced by the new, added function of the composites, which is the ability to be monitored via electrical resistance change (piezoresistivity). This is further explained in several research papers that are cited in the manuscript, e.g. [13,14,19], etc.

Added cost to attain this new material function is multiple-fold, including manufacturing process-, composites dimensional-, resin temperature- and wt.% CNTs addition- different parameters. Fig. 12a shows an example of calculation cost for the manufacturing of an 800 mm × 800 mm plate with three different processes, while resin injection temperatures used was 70 °C for VARI and RTM processes. For the case of 1.0 wt.% CNTs composites, added cost to attain this new material function is approximately 34.26% for the Hand Lay-up, 27.42% for VARI and almost 22.17% for RTM manufacturing method. Of course, the lower the CNT content used in the composite, the lower the added cost percentages to attain the new function should be. For example, for the case of addition 0.5 wt.% CNTs, then the added cost to attain piezoresistivity would be 28.06%, 22.46% and 18.16% for the different above manufacturing processes, respectively. The upper and lower limits for this added cost is manufacturing process-specific and can be seen in Fig. 12b. In the figure one can notice the mechanical performance pros and cos of the CNTs addition in the matrix of the composite. Due to the low manufacturing cost of a GFRP plate by employing the Hand Lay-up method, this increased added cost is mainly due to purchase of CNTs and its dispersion technique. The lower the

CNTs purchase cost becomes, the lower the total cost of the composites would become. By employing the automated manufacturing processes VARI and RTM, it can be seen that added cost is much lower (varying from 18% to 22%) for the most expensive process in the present study, that is the RTM process. Please notice that the present cost functions were developed for Laboratory scale; in real, industrial conditions a large number of composite structures is supposed to be manufactured. This will further suppress manufacturing cost per part, thus it is the authors' opinion that added cost to attain multi-functionality via dispersion of CNTs will be further decreased to approximate 10% of total manufacturing cost.

Adding the piezo-resistivity function to GFRPs via the CNTs dispersion in the resin seems to be the unique method for this period of time. Addition of carbon black particles were also used in another research work to attain this function [19]; it was esteemed with limited success in terms of piezoresistivity, as carbon black particles seems to have less contacting points between them to establish conductive paths in the resin's structure. This makes the monitoring of such composites via electrical current measurements very difficult to almost impossible.

## 8. Selection of optimal parameters

In previous sections, it was described that VARI process was employed since it attains relatively high dimensional accuracy and quality as well as low manufacturing cost. Considered VARI manufacturing parameters were plate geometrical dimensions, resin injection temperature and CNTs content reinforcing resin. It was shown that as GFRP plate dimensions increase the coupon cost is diminishing, mainly because the larger the plate area the bigger the number of the manufactured coupons and therefore the lower coupon cost. Infusion temperature affects mould filling time; upper threshold of 80 °C for gelation point should not be exceeded, and therefore resin injection temperature (70 °C), that minimizes mould filling time and does not lead to resin gelation is selected as optimum injection temperature. An enhancement of the mechanical performance was expected initially, with the addition of CNTs inside the matrix. Tensile test results on composites with different percentages of CNT doped resin showed that modulus of elasticity $E$ and tensile strength $R_m$ values were continuously increased, while strain energy density $W$ and elongation at fracture $A_m$ were decreased with increasing CNT content. Fig. 13 shows cost calculation results over quality indices' change that indicates ability change for mechanical performance.

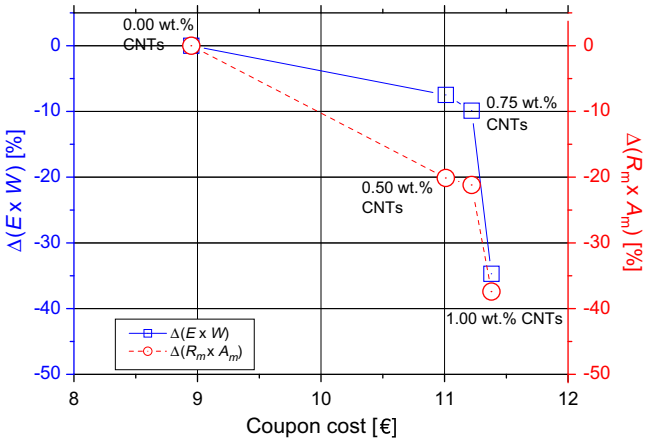


**Fig. 13.** Quality indices change as a function of coupon cost for various CNT concentrations.

Though quality is continuously decreasing with increasing CNT content, the ability of the new materials to be monitored via electrical resistance change method cannot be quantified in this quality index. As the 0.50 wt.% concentration has marginally passed the percolation threshold in the resin, addition of 0.75 wt.% is considered essential to enhance the ability to be effectively monitored.

## 9. Conclusions

Evaluation of different manufacturing parameters has been performed to identify optimum processing parameters for the production of innovative, carbon nanotube – based polymer composites through the most efficient manufacturing processes known so far.

A fully-parametric cost model has been developed to calculate respective manufacturing cost by taking into account each individual sub-process. Several case studies has been considered, including (a) manufacturing process, (b) geometrical dimensions, (c) carbon nanotubes concentration in the epoxy resin and finally (d) modified resin infusion temperature.

Evaluation of the produced hybrid composites has been performed on combined aspects of mechanical performance and manufacturing cost. For the present study, added manufacturing cost to produce the nano-reinforced composites was attributed to increase the strength properties on the expense to the ductility properties. The real merit of the CNTs addition seems not to be the mechanical performance but the added function of piezo-resistivity; the ability of being monitored via electrical resistance change is an unambiguous benefit.

Almost 20% of the nano-reinforced composite's total cost is attributed to attain this new function, when manufactured with the automated RTM process. Added costs for manufacturing the same nano-reinforced product are approximate 25% and more than 30% for the VARI and Hand Lay-up processes, respectively.

## Acknowledgements

The authors would like to acknowledge the Advanced Composites Laboratory of Hellenic Aerospace Industry for manufacturing the investigated materials and especially Dipl. Ing. A. Meletis for fruitful discussions over the manufacturing processes.

## References

[1] Kaufmann M, Zenkert D, Ekermo M. Cost/weight optimization of composite prepreg structures for best draping strategy. Compos Part A 2010;41:464–72.
[2] Kaufmann M, Zenkert D, Wennhage P. Integrated cost/weight optimization of aircraft structures. Struct Multidiscip Optimiz 2010;41:325–34.
[3] Kassapoglou C, Dobyns AL. Simultaneous cost and weight minimization of postbuckled composite panels under combined compression and shear. Struct Multidiscip Optimiz 2001;21:372–82.
[4] Kassapoglou C. Minimum cost and weight design of fuselage frames. Part B: Cost considerations, optimization, and results. Compos: Part A 1999;30:895–904.
[5] Gantois K, Morris AJ. The multi-disciplinary design of a large-scale civil aircraft wing taking account of manufacturing costs. Struct Multidiscip Optimiz 2004;28:31–46.
[6] Kaufmann M, Zenkert D, Mattei C. Cost optimization of composite aircraft structures including variable laminate qualities. Compos Sci Technol 2008;68:2748–54.
[7] Bernet N, Wakeman MD, Wakeman P-E, Manson J-AE. An integrated cost and consolidation model for commingled yarn based composites. Compos: Part A 2002;33:495–506.
[8] Verrey J, Wakeman MD, Michaud V, Manson J-AE. Manufacturing cost comparison of thermoplastic and thermoset RTM for an automotive floor pan. Compos: Part A 2006;37:9–22.
[9] Ye J, Zhang B, Qi H. Cost estimates to guide manufacturing of composite waved beam. Mater Des 2009;30:452–8.
[10] Bader MG. Selection of composite materials and manufacturing routes for cost effective performance. Compos: Part A 2002;33:913–34.

[11] Park CH, Lee WI, Han WS, Vautrin A. Simultaneous optimization of composite structures considering mechanical performance and manufacturing cost. Compos Struct 2004;65:117.
[12] Cai Z. Estimation of the permeability of fibrous preforms for resin transfer moulding processes. Compos Manuf 1992;3:251–7.
[13] Thostenson ET, Chou TW. Real-time in situ sensing of damage evolution in advanced fiber composites using carbon nanotube networks. Nanotechnology 2008;19:215713.
[14] Thostenson ET, Chou TW. Carbon nanotube networks: Sensing of distributed strain and damage for life prediction and self healing. Adv Mater 2006;18:2837–41.
[15] Schulte K, Baron Ch. Load and failure analyses of CFRP laminates by means of electrical resistivity measurements. Compos Sci Technol 1989;36:63–76.
[16] Gao L, Thostenson ET, Zhang Z, Chou TW. Sensing of damage mechanisms in fiber-reinforced composites under cyclic loading using carbon nanotubes. Adv Funct Mater 2009;19:123–30.
[17] Fiedler B, Gojny FH, Wichmann MHG, Bauhofer W, Schulte K. Can carbon nanotubes be used to sense damage in composites? Annales de Chimie: Science des Materiaux 2004;29:81–94.
[18] Gojny FH, Wichmann MHG, Fiedler B, Kinloch IA, Bauhofer W, Windle AH, et al. Evaluation and identification of electrical and thermal conduction mechanisms in carbon nanotube/epoxy composites. Polymer 2006;47(6):2036–45.
[19] Boeger L, Wichmann MHG, Meyer LO, Schulte K. Load and health monitoring in glass fibre reinforced composites with an electrically conductive nanocomposite epoxy matrix. Compos Sci Technol 2008;68:1886–94.
[20] Muto N, Arai Y, Shin SG, Matsubara H, Yanagida H, Sugita M, et al. Hybrid composites with self-diagnosing function for preventing fatal fracture. Compos Sci Technol 2001;61:875–83.
[21] Wichmann MHG, Buschhorn ST, Boeger L, Adelung R, Schulte K. Direction sensitive bending sensors based on multi-wall carbon nanotube/epoxy nanocomposites. Nanotechnology 2008;19:475503.
[22] Alexopoulos ND, Eleftheriou J, Asimakopoulos A, Georgiou Ch, Marioli-Riga Z. Piezo-resistivity and mechanical properties of glass fiber reinforced coupons using carbon nanotube CNT doped resin. In: Proceedings of 18th European conference on fracture (ECF18), Dresden, Germany; 30 August–03 September 2010.
[23] Halley PJ, Mackay ME. Chemorheology of thermosets – an overview. Polym Eng Sci 1996;36(5):593–635.
[24] Ivanov E, Kotsilkova R, Krusteva E, Logakis E, Kyritsis A, Pissis P, et al. Effects of processing conditions on rheological, thermal, and electrical properties of multiwall carbon nanotube/epoxy resin composites. J Polym Sci Part B: Polym Phys 2011;49:431–42.
[25] Cueto E, Monge R, Chinesta F, Poitou A, Alfaro I, Mackley MR. Rheological modeling and forming process simulation of CNT nanocomposites. Int J Mater Form 2010;3:1327–38.
[26] Song YS. Multiscale fiber-reinforced composites prepared by vacuum-assisted resin transfer molding. Polym Compos 2007;28:458–61.
[27] Hubert P, Johnston A, Poursartip A, Nelson K. Cure kinetics and viscosity models for Hexcel 8552 epoxy resin. In: Proceedings of international SAMPE symposium and exhibition, vol. 46; 2001. p. 2341–54.
[28] Prolongo SG, Gude MR, Ureña A. Rheological behaviour of nanoreinforced epoxy adhesives of low electrical resistivity for joining carbon fiber/epoxy laminates. J Adhes Sci Technol 2010;24:1097–112.
[29] O'Guin MC. The complete guide to activity-based costing. Prentice Hall; 1991.
[30] Thostenson ET, Chou TW. Scalable processing techniques for nanotube-based polymer composites. In: Proceedings of 16th international conference on composite materials - ICCM 16, Kyoto, Japan; July 2007.
[31] Seyhan AT, Tanoglu M, Schulte K. Tensile mechanical behaviour and fracture toughness of MWCNT and DWCNT modified vinylester/polyester hybrid nanocomposites produced by 3-roll milling. Mater Sci Eng A 2009;523(1–2):85–92.
[32] Alexopoulos ND, Pantelakis SpG. A new quality index for characterizing aluminum cast alloys with regard to aircraft structure design. Metal Mater Trans A 2004;35A(1):301–8.
[33] Alexopoulos ND. Low-alloy TRIP steels: evaluation of the mechanical performance with regard to material's design requirements in the automotive industry. Steel Res Int 2006;77(2):129–38.
[34] Alexopoulos ND, Apostolopoulos ChAlk, Papadopoulos MP, Pantelakis SpG. Mechanical performance of BStIV grade steel bars with regard to the long-term material degradation due to corrosion damage. Constr Build Mater 2007;21(6):1362–9.
[35] Vasile C, Kulshreshtha AK. Liquid moulding process. Handbook Polym Blends Compos 2002;2:53–63.
[36] Kushima A, Lin X, Yip S. Commentary on the temperature-dependent viscosity of supercooled liquids: a unified activation scenario. J Phys: Condens Matter 2009;21(50):504104.
[37] Khoun L, Centea T, Hubert P. Characterization methodology of thermoset resins for the processing of composite materials – case study. J Compos Mater 2010;44:1397–415.
[38] Boccard A, Lee WI, Springer GS. Model for determining the vent locations and the fill time of resin transfer molds. J Compos Mater 1995;29(3):306–33.
[39] Schilde C, Nolte H, Arlt C, Kwade A. Effect of fluid–particle-interactions on dispersing nano-particles in epoxy resins using stirred-media-mills and three-roll-mills. Compos Sci Technol 2010;70:657–63.